International Conference on Artificial Reality and Telexistence
Eurographics Symposium on Virtual Environments (2017)
R. Lindeman, G. Bruder, and D. Iwai (Editors)

Fast and Accurate Simulation of Gravitational Field of Irregular-shaped Bodies using Polydisperse Sphere Packings

Abhishek Srinivas , Rene Weller & Gabriel Zachmann

Computer Graphics & Virtual Reality Group, University of Bremen, Germany

Abstract

Currently, interest in space missions to small bodies (e.g., asteroids) is increasing, both scientifically and commercially. One of the important aspects of these missions is to test the navigation, guidance, and control algorithms. The most cost and time efficient way to do this is to simulate the missions in virtual testbeds. To do so, a physically-based simulation of the small bodies' physical properties is essential. One of the most important physical properties, especially for landing operations, is the gravitational field, which can be quite irregular, depending on the shape and mass distribution of the body. In this paper, we present a novel algorithm to simulate gravitational fields for small bodies like asteroids. The main idea is to represent the small body's mass by a polydisperse sphere packing. This allows for an easy and efficient parallelization. Our GPU-based implementation outperforms traditional methods by more than two orders of magnitude while achieving a similar accuracy.

CCS Concepts

•***Computing methodologies*** → *Real-time simulation;* •***Human-centered computing*** → *Virtual reality;* •***Applied computing*** → *Aerospace;*

1. Introduction

Recently, there has been a surge in space missions to small celestial bodies (such as asteroids and comets). Major space agencies such as NASA, ESA, and JAXA have already conducted small bodies missions and have many more missions planned for the future. For instance, JAXA landed the Hayabusa probe on asteroid Itokawa in 2005 and successfully returned collected asteroid samples in 2010. In 2014 ESA's Rosetta spacecraft orbited the Comet 67p and later landed the Philae probe on the nucleus. NASA is currently planning for a sample return mission to asteroid Bennu. Conducting research missions to these bodies is crucial for understanding the origins of the solar system. It will also help for future space missions, where resources (e.g., water) can be mined on-site and utilized in synthesizing propellants. Furthermore, there is increasing commercial interest in such missions, in order to mine other materials (e.g., nickel-iron) for the mid-term future by private companies.

One of the most important parts of preparation for these missions is to test the navigation, guidance and control algorithms to avoid the damage of the expensive hardware in the real world missions. These algorithms are quite complex for normal planetary missions. The situation is aggravated for small bodies missions, mainly because of the limited ground-truth data available. Additionally, spacecraft are becoming more and more autonomous due to the complexity of the proximity and surface operations on small bodies, and due to the long distances that prevent manual control, which increases the complexity of the algorithms on board the spacecraft. Furthermore, the number of mission concepts for any given mission scenario is very large. Therefore, it is crucial to test these algorithms thoroughly. A cost effective and time efficient way is to simulate the mission in a virtual testbed, which provides a tool for quickly testing and optimizing complex algorithms under different scenarios. To do so, the virtual testbed must simulate physical aspects of the space mission environment such as solar pressure, complex rotation of asteroids, asteroid surface features, asteroid gravity, etc., which usually dominates the computation time. In this paper, we focus on the simulation of the gravitational field, because it is a crucial aspect, especially in the close proximity and landing phases. Furthermore, it takes a considerable portion of the overall time needed to run one simulation step. For instance, it is required for planning optimal trajectories but also for the physically-based world simulation.

For a long time, the computation of the gravitational field usually done outside the Brillouin sphere: this is a sphere originating at the center of mass and encompassing the body (see Figure 1). This works well for fly-by missions or almost spherical bodies but it is not suitable for landing missions on irregularly shaped bodies. During the past years, a few methods were proposed to compute the gravitational field closer to the surface. In the next section, we provide a review of these methods.

In this paper, we present a novel algorithm that contributes the following advantages to the field of gravitation field computation of small bodies:

DOI: 10.2312/egve.20171361

- Our algorithm is suitable for arbitrarily shaped bodies.
- It easy to implement.
- It can be perfectly parallelized.
- It is more than two orders of magnitude faster than previous algorithms while maintaining a similar accuracy.
- It supports arbitrary mass distributions inside the asteroid.

The main idea of our algorithm is to represent the asteroid by a polydisperse, space-filling sphere packing, which simplifies a number of calculations. Obviously, there are always small voids between the spheres. We present several different strategies to deal with these voids to improve the accuracy of our algorithm. We also present the parallelized version, which we have implemented using CUDA. For evaluation, we computed the gravitational field of several asteroids for which there are real-world models available. Unfortunately, ground truth data from real gravity measurements for these asteroids does not exist. We compared our algorithm to a polygon-based approach that is known for the best accuracy available. However, this method supports only uniform mass density distributions, hence we restricted our comparisons also to this kind of mass distributions. Please note that our algorithm also supports arbitrary mass distributions, which is important since the mass distribution inside asteroids is probably highly non-uniform. Our results show a high accuracy and a good performance even in very close proximity to the ground.

2. Previous work

Currently, virtual test beds are becoming a significant tool for testing various aspects of space explorations. These aspects can be as diverse as lunar surface operations to proximity and landing operations on asteroids. For instance, the LSOS simulator [NBC*08] which provides a virtual test bed for design and planning of the lunar space missions to land and return astronauts to the moon. The JPL multi-mission simulation toolkit Darts/Dshell [LJ09] is used for modeling spacecraft dynamics, devices, and subsystems, and is in use by interplanetary and science-craft missions such as Cassini, Galileo, SIM, and Starlight. Regarding small bodies mission simulators, there is SEAS [BCJ*11] from JPL, which provides high-fidelity models of the environment, deployed systems and interactions between them under realistic operational scenarios. All of these simulators have a simple algorithm for computing the gravitational field.

A major challenge for the simulation of small bodies missions in virtual environments is the modeling and simulation of the gravity field of irregularly, i.e. non-spherical, shaped bodies. The existing methods for modeling the gravitational field of irregular-shaped bodies can be classified into three categories: polyhedral gravitational methods, spherical harmonic methods, and mascons (finite mass elements) methods (distribution of finite mass elements). Most of the current state of the art small-bodies virtual test beds such as SEAS [BCJ*11] use a polyhedral gravitational model. Polyhedral models, such as the one presented in [WS96], give a closed form solution for a closed polyhedron shape with a uniform mass distribution. However, this method is computationally expensive for high-resolution shapes.

In the case of spherical harmonics models, the most common

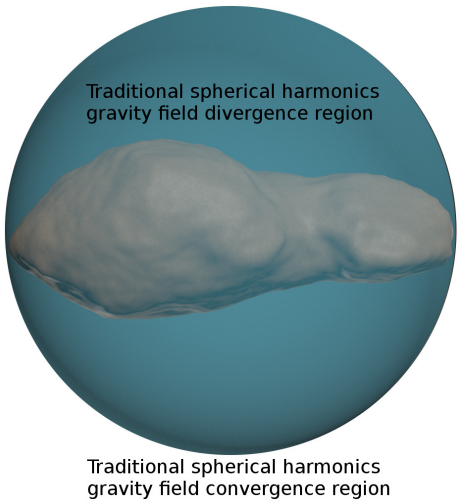

Figure 1: *Brillouin sphere, here shown with the example of asteroid Toutatis. The traditional representation of gravity fields using spherical harmonics does not converge inside this sphere. So spherical harmonics are an unsuitable representation for close proximity operations or the descent phase of an asteroid mission.*

and computationally fast method is the traditional exterior spherical harmonics method. However, the convergence of the spherical harmonics model inside the Brillouin sphere (sphere originating at the center of mass and encompassing the body (see Figure 1) is not guaranteed and hence this model is unsuitable for regions within the Brillouin sphere. There are certain methods which extend the spherical harmonic methods in order to overcome the low accuracy for close-proximity operations. One such method is spherical harmonics expansion method [TS14], which is applicable for variable density bodies and the model also converges inside the Brillouin sphere. However, generating a configuration of this model is highly time-consuming and implementing the model is complex.

The mascons-based models generally have a number of point mass concentrations and use the simple computation of the sum of point masses gravitational acceleration to approximate the gravitational field of irregular-shaped bodies. Masons-based methods usually need a large number of point masses to achieve an acceptable level of accuracy [RA12]. Currently, some mascons-based methods have shown potential in decreasing the computational time while still maintaining good gravitational field accuracy as presented in [Tar16] and [PWB08]. Typical shapes for the masses are either voxels or spheres. [PWB08] used both, cubes and spheres as mascons with simple space filling arrangements. However, they use batch least squares filter to assign masses to these mascons, which is extremely slow. [Tar16] compares a number of mascon-models and some of them had a relative accuracy of about 1% compared to the polygonal method close to the surface of an asteroid.

Most of the mascon models compute the gravitational acceleration in a similar way, the differences are in mascons distribution, representation and computational time for the model generation. This paper's method follows the same general principle of the mascons-model presented in [Tar16], where the authors fill the irregularly-shaped body with a number of spheres by using differ-

ent sphere arrangement methods. However, we use a more efficient sphere filling algorithm and better mass distribution methods in terms of estimated errors. Computing the acceleration at any given point is trivial as shown in the equation 2, since each sphere can be considered a point mass.

3. Our Approach

Our algorithms reconsider the mascon model as a way to model the gravity field of irregular-shaped bodies. The main objective is to improve the current mascon models by using better mascon representation and distribution for better computational efficiency and higher accuracy. In particular, we are interested in the accuracy of the gravitational field estimated by our model *inside* the Brillouin sphere and computational performance of our model w.r.t gravitational acceleration computation.

3.1. Mascon Model Basics

The main idea of the mascons model is to subdivide the body into smaller parts, the mascons. The overall gravitational pull can be computed by an integration over all these mascons (point masses). Obviously, it is important that the gravitational accelerations for the mascons should be easy to compute. Therefore, spheres are an ideal mascon shape, because computing the gravitational acceleration at any given point is trivial. For a single sphere s with mass M and a gravitational constant G, we get at point $\mathbf{x}$ the gravitational acceleration

$$\mathbf{g}(\mathbf{x}) = \frac{GM}{\|\mathbf{r}\|^3}\mathbf{r} \tag{1}$$

with $\mathbf{r} = \mathbf{c} - \mathbf{x}$ the vector between the point and the sphere's center.

For a complete sphere packing S with n spheres with individual centers $\mathbf{c}_i$ and masses M_i, $i = 1,\ldots,n$, we get an accumulated gravitational acceleration at point x of:

$$\mathbf{g}(\mathbf{x}) = \sum_{i=1}^{n} \frac{GM_i}{\|\mathbf{r_i}\|^3}\mathbf{r_i} \tag{2}$$

with $\mathbf{r_i} = \mathbf{c_i} - \mathbf{x}$. This makes it appealing to use sphere packings to represent the bodies.

The computation of equation 2 can be easily parallelized:

Algorithm 1: gravity(query point x, sphere packing S)

in parallel forall *spheres* $s_i \in S$ **do**
  $r_i = c_i - x$
  $g_i(x) = \frac{GM_i}{\|\mathbf{r_i}\|^3}\mathbf{r_i}$
parallel scan over all g_i computes $g(x) = \sum_{i=1}^{n} g_i(x)$

Each thread computes the acceleration for a single mascon and a parallel scan sums up the individual gravitational accelerations. There are two main challenges with the mascons model: the first one is the computation of an appropriate space subdivision, i.e. the choice of the mascons representation and their arrangement; the second one is the assignment of the masses to the mascons. We will address these topics in the following sections.

3.2. Mascons Arrangement and Representation

As mentioned above, we decided to use a sphere representation for the mascons. In order to represent the volume of the small body as accurate as possible, we require an adequate sphere packing for it. According to the Kepler conjecture, uniform spheres can cover at most 75% of an object's volume. Hence, we decided to use polydisperse sphere packings. Fortunately, Algorithm 1 accepts such kinds of spherical representations.

The *Protosphere* [WZ10] extends the idea of Apollonian sphere packings to arbitrary 3D objects. It produces space filling sphere packings using a greedy algorithm, i.e. first, the largest sphere is fitted into the 3D body, then the second largest into the remaining space etc. Protosphere is faster and more robust compared with spheres packing methods presented in [Tar16] that place spheres only at fixed positions of a grid and it has better filling fractions. An other advantage is that the greedy choice of the algorithm leads automatically to a level-of-detail representation for the gravitation computation. Compared to the other methods, Protosphere generates real sphere packings, i.e. the spheres do not overlap and they are all completely inside the 3D container. Figure 2 shows the polygonal mesh of the asteroid Itokawa and a respective sphere packing generated by Protosphere.

Basically, the algorithm also supports the definition of minimum and maximum sphere sizes. Moreover, it would be possible to include other optimization criteria to influence the arrangement of the spheres in the packing. However, in this paper we used the standard greedy implementation and leave the investigation of the influence of the arrangement of spheres for further investigations. With the standard algorithm Protosphere generates sphere packing fractions of more than 90% for most of the asteroid shape models with only 100k spheres. This packing density is more than 5% higher than that of competing algorithms [Tar16]. As a result, this should improve the gravitational field estimation accuracy.

3.3. Mascon Mass Distribution

Once the spheres arrangement is generated, which fills the polyhedral model of the small body, the next step is to assign masses to these spheres so that the mascon model is able to estimate the gravitational accelerations. The total mass of an asteroid M can be estimated by using the method described in [KF13]. Obviously, the summed mass of all mascons should equal the total estimated mass of asteroid M. Assigning the masses to the mascons is a highly non trivial task, especially in case of sphere packings, because of the voids between the mascons. Even if we receive a filling rate of $> 90\%$ the missing volume may lead to significant errors. The Protosphere algorithm uses a greedy approach, hence, a large potion of the small body may be covered by a single large sphere while other parts are filled with many smaller spheres. This results in an unequal distribution of the voids. In order to overcome this drawback, we propose several strategies.

3.3.1. Volume proportional method (VP)

The most simple method is to ignore the voids and simply assign the masses proportional to each sphere's volume. More precisely, we compute the total volume V_S for a sphere packing S with:

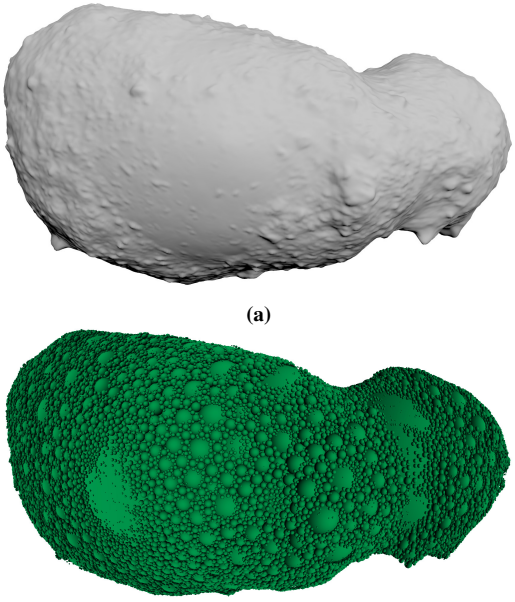

(a) **(b)**

Figure 2: *(a) Polygonal mesh of Itokawa with 200 thousand faces and (b) respective sphere-packings (100 thousand) of the above mesh generated using the Protosphere algorithm with default parameters.*

$$V_S = \sum_{s_i \in S} v_i \tag{3}$$

where v_i are the volumes of the spheres. This allows us to simply compute the mass m_i of each sphere by:

$$m_i = M \frac{v_i}{V_S} \tag{4}$$

Obviously, the sum of the masses of all mascons is exactly M. However, this method does not take into account the sphere distribution.

3.3.2. Bulk density uniformity method (BDU)

The Protosphere algorithm generates polydisperse spheres greedily. As a consequence, regions consisting of larger spheres have larger packing fraction compared with regions consisting of smaller spheres. Considering that the all the spheres have the same mass density, than the regions with larger spheres have a higher average mass density (bulk density) compared with regions with smaller spheres because of a larger amount of gaps (see figure 3). Therefore, to maintain the homogeneity of bulk density the straight forward way is to reduce densities of the larger spheres and increase the densities of the smaller spheres. In [Tar16] this is partially achieved by only reducing density of largest sphere and by increasing the density of the all the other spheres equally.

We improved this method by changing the densities of *all* spheres with regard to there sizes (volumes). To do that, we sort the spheres by their volumes v_i, where v_1 is the largest and v_n is the smallest sphere. Let V_p be the volume of the polygonal model of the asteroid. We recursively define for each sphere $V^p_{i-1} = V^p_i - v_i$. This defines a reduction factor $f_i = V^p_i / V^p_{i-1}$ for each spheres. We use this factor to reduce the particular volume v_i of each sphere. Obviously, the resulting mass distribution

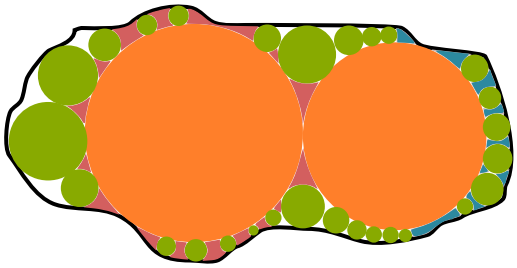

Figure 3: *2D representation of an asteroid sphere packings with different bulk regions. Red region (consisting of a large sphere) has higher bulk density compared with blue region (consisting of smaller spheres)*

$$M_r = \sum_{s_i \in S} \frac{f_i v_i}{V_p} M \tag{5}$$

is smaller than M. Hence, we normalize the masses of the spheres by a factor of M/M_r. This results in variable mass density: spheres with larger volume having lower density than smaller spheres. As a consequence, we achieve a much more uniform bulk density compared with the volume proportional method and as a result, we can expect a better gravitational field estimation accuracy.

3.3.3. Delta radius increase method (DRI)

The VP adapts the masses of the mascons to match the bodies total mass but it does not consider the voids between the spheres. In this method we reduce the gaps by increasing the mascons volumes. More precisely, we will increase the radii r_i of the spheres $s_i \in S$, $i = 1, \ldots, n$ by a constant δ so that their summed volumed matches the bodies total volume:

$$V_p = \sum_{i=1}^{n} \frac{4\pi(r_i + \delta)^3}{3} \tag{6}$$

The constant δ can be easily computed by solving Equation 8. This leads to a small overlap of the spheres, however, it does not affect the computations of Algorithm 1. The final masses of the mascons are computed by:

$$m_i = M \frac{v'_i}{V_S} \tag{7}$$

where v'_i are the increased volumes

$$v'_i = \frac{4\pi(r_i + \delta)^3}{3} \tag{8}$$

of each sphere s_i. Obviously, we get:

$$M = \sum_{i=1}^{n} m_i \tag{9}$$

In this method we assume that the total volume of the spheres is equal to the total volume of the polygonal model. Actually, it is possible to over- or underestimate the volume V_p which would lead to larger or smaller, respectively δs. However, our experiments have shown that adopting the sphere packing's volume to V_p leads to the best results (see Figure 4. Figure 5 additionally shows the size comparison of normal spheres with the increased spheres using the DRI method for the asteroid Eros).

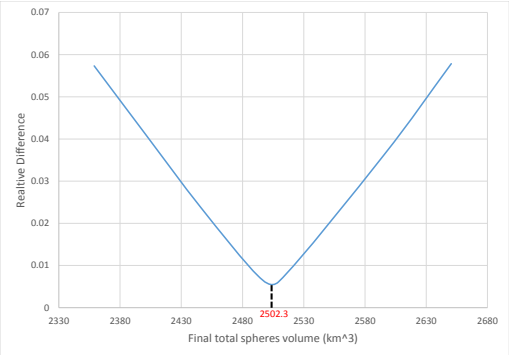

Figure 4: *Plot of total relative differences of the estimated gravitational field at an altitude of 1m from the Eros asteroid polygonal model surface w.r.t to the different final total volume of the spheres considered for solving δr. The minimum difference is obtained at the final total volume of spheres equal to the actual volume of the Eros asteroid polygonal model 2502.3km^3*

3.3.4. Delta percentage volume increase method (DPVI)

An advantage of the DRI method is that it implicitly improves the density distribution of the spheres: The spheres radii are increased by a fixed amount, hence the *relative* increase of the sphere volume for smaller spheres is considerably higher than for the larger spheres. This is a favorable consequence as the current bulk densities in the regions of smaller spheres increases, which previously had lower bulk densities than in regions consisting of larger spheres. Another consequence is the decrease in volume of the gaps closer to the smaller spheres, which have a higher proportion of empty volume in their vicinities.

However, these favorable properties can be further improved by assigning even more volume to smaller spheres. A simple heuristic is to increase the volumes of the spheres by a fraction proportional to their respective radii instead of using a constant radius increase for all spheres.

Let v_i be the volume of sphere s_i. We increase the volumes v_i of each sphere by a constant fraction x/r_i of the current volume v_i, where x is a constant factor which remains the same for all the spheres. x is obtained from equation 10, which is derived by considering the fact that total volume of the sphere packings after increasing the volume of all the spheres is equal to the volume of the polygonal model V_p.

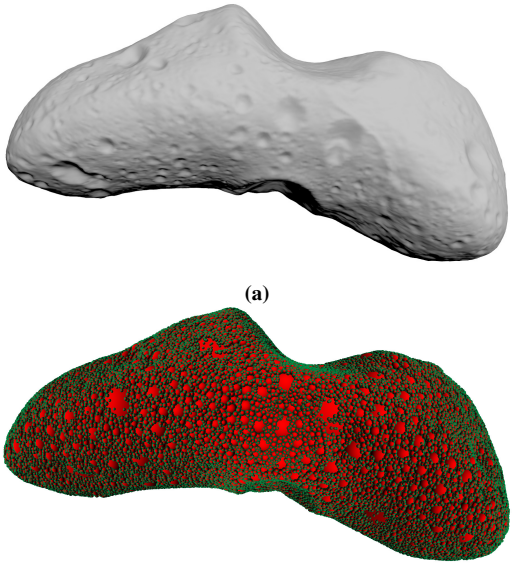

Figure 5: *(a) Polygonal mesh of Eros with 200 thousand faces. (b) Size comparison of the default spheres (red spheres) generated by the Protosphere and spheres with larger radius (green spherical enclosures) after applying the DRI method for Eros asteroid shape model*

$$x = \frac{V_p - \sum_{i=0}^{n-1} v_i}{\sum_{i=0}^{n-1} \frac{v_i}{r_i}} \tag{10}$$

The individual radius increase δr_i of each sphere s_i can be obtained by solving the cubic equation 11

$$\frac{4\pi(r_i + \delta r_i)^3}{3} = V_i + \frac{V_i x}{r_i} \tag{11}$$

Similar to the final step of the DRI method, masses to these increased radii spheres are assigned by considering a uniform density equal to the mean density of the given small body.

4. Results

We have implemented our algorithm, including the different mass assignment methods, using CUDA. We tested the performance as well as the quality of the computed gravity fields. We used several available polygonal asteroid model with a reasonable polygon resolution, namely, Itokawa [RJM*08], Lutetia [T.L13] and Eros [R.W08]. Itokawa and Eros have very similar non-spherical shapes with contrasting volumes. On the other hand, Lutetia has almost spherical shape with a larger volume compared with the above-mentioned asteroids. For all these asteroids we generated sphere packings in several resolutions up to 1 million of spheres. All computations were done using double precision.

4.1. Accuracy

In order to measure the accuracy of our model, we compute gravitational field for points equally spaced in longitude and latitude enclosing the asteroid body at different altitudes from the surface similar to procedure presented in [Tar16]. We consider primarily points inside the Brillouin because for points outside this sphere, the exterior spherical harmonics model can be used. The spherical harmonics model is computationally inexpensive and is accurate enough to be considered for orbital operation purposes and for simulations in virtual test beds. We measured the gravity field at two different altitudes i.e. close to the surface (1m) and at an altitude of 100 meters. Unfortunately, ground truth data from real world gravity field measurements of these asteroid is not available. Hence, we measured the relative differences to the polygonal model (from now onwards term relative difference is used instead of relative difference of gravitational model or accelerations w.r.t to polygon model for convenience), even if the polygonal model is just an approximation of the real asteroid's shape and introduces its own error. According to [MKA*02], the error of the high resolution polygonal model for Eros is about 1%. In smaller asteroids such as Itokawa, these errors could be higher due to large mass concentrations such as dust rubbles. The figures 6 and 7 show the relative root mean square differences of our algorithm for Lutetia and Itokawa compared to the polygonal model w.r.t to gravitational accelerations. Figure 8 shows the distribution of relative differences on the Eros surface using the traditional box plots, which clearly shows that maximum, mean and other quartiles relative differences decrease with an increasing number of spheres. We observed similar trends of surface relative difference distribution for the surfaces of Itokawa and Lutetia.

The relative differences of all our methods are less than 2% even with only 80 thousand spheres compared to the polygonal model. However, for all our methods we observe that the relative difference decreases with an increasing number of spheres. DRI and DPVI have almost the same accuracy and they perform best among all methods. The accuracy is almost three times better than that of the VP and the BDU method for all asteroids. Even though the DRI and DVPI methods produce overlapping spheres, the relative differences are still lower than non-overlapping spheres methods (VP and BDU). This shows that the relative differences due to gaps are much higher than the errors produced by overlapping spheres. Similar trends are observed for all the methods at altitude of 100 meters as well.

However, DRI and DPVI methods also have estimated differences that are lower than the best method reported in [Tar16] by using only one third of the number of spheres. Please note that the above comparison is only applicable inside the Brillouin sphere.

Additionally, we investigated the relation between the accuracy and the altitude. For this evaluation, we included also points outside the Brillouin sphere up to 1 km above the ground (see Figure9). In the case of Eros, the differences for all methods decrease gradually with an increasing altitude. Almost the same trend is observed for Lutetia (9b) as well except that rate of decrease is lower for VP and BDU methods. The rate of decrease remains almost consistent for DRI and DPVI methods irrespective of the asteroids. The relation between the differences and altitudes with regard to BDU and VP

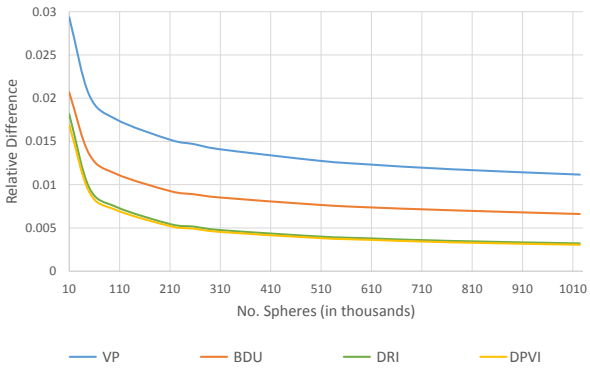

(a) *1 meter*

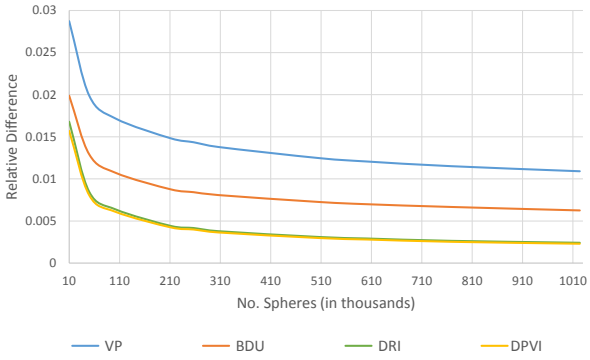

(b) *100 meters*

Figure 6: *RMS relative differences of the estimated gravitational accelerations at altitudes (a) 1 meter (b) 100 meters from the Lutetia surface w.r.t different number of sphere packings for different methods*

methods seems to be characteristic of the asteroid shape as both the Eros and Itokawa have similar plots due to the similarity in their shapes. On the other hand, Lutetia has different characteristic as its shape model is contrasting with the Eros and Itokawa shape models. Also, different asteroids have different accuracies close to the surface and this also seems to be characteristic of the shape of the asteroids. We will further investigate this characteristic in the future. Even though, decreasing rates reported in [Tar16] seems to be higher, however, the difference is still higher than DPVI and DRI method within the Brillouin sphere.

4.2. Performance

We performed the computation of the gravitational fields for Itokawa for several polygon and sphere resolutions reaching from a few thousands up to one million polygons and spheres, respectively. We used only Itokawa because we only have such high polygonal models for this asteroid. The shape of the asteroid does not influence the computation time, hence, the timings can be directly transferred to the other asteroids. We used our parallel implementation of our algorithm and we additionally parallelized the polygonal algorithm to provide a fair comparison (The parallelization for the polygonal algorithm was done for the faces and edges). All computations were performed on a Nvidia Quadro K1100M GPU.

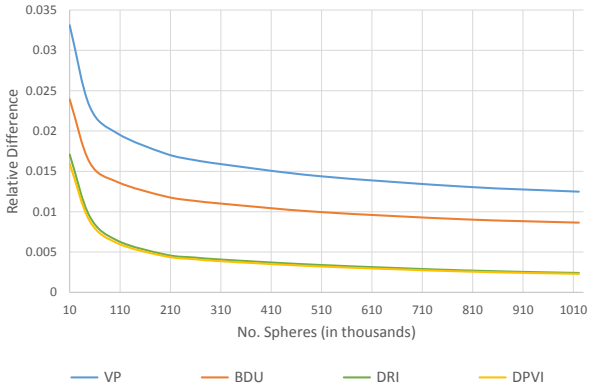

(a) *1 meter*

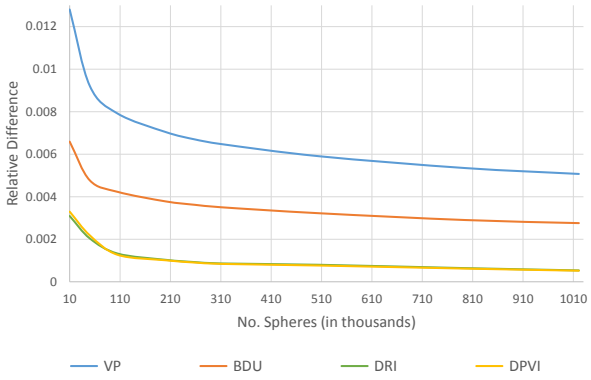

(b) *100 meters*

Figure 7: *Plots of RMS relative differences of the estimated gravitational accelerations at altitudes (a) 1 meter (b) 100 meters from the Itokawa surface w.r.t different number of sphere packings for different methods*

The query time for a single point of the polygonal algorithm is 130 milliseconds for the highest resolution model (1 million of polygons) and less than 1 millisecond for the sphere packing based methods. The overall performance gain of our algorithm is by a factor of around 20 (see Figure 10). The accuracy difference, especially close to the ground (1m), is less than 1.0% and thus, in the reach of the accuracy of polygonal models [MKA*02] for all asteroid shapes we have tested. Actually, this accuracy threshold can be reached with a much smaller number of spherical mascons, i.e., we need a much smaller number of spheres to obtain the same accuracy which further increases the performance gain by a factor of 200-300. Moreover, the number of spheres required to gain a certain level of accuracy is independent of number of polygons of the polygonal model (see Figure 11).

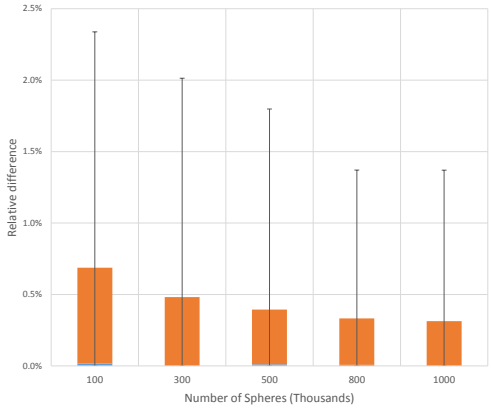

Figure 8: *Box plots of relative differences of DPVI method and polyhedral model using Eros asteroid shape model*

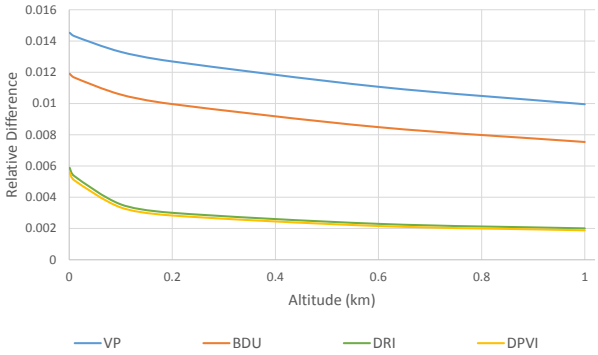

(a) *Eros*

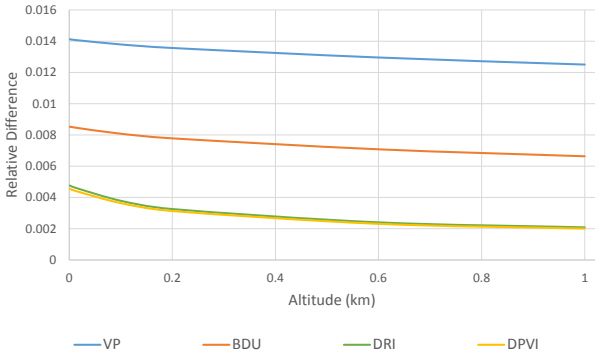

(b) *Lutetia*

Figure 9: *Plot of RMS relative differences of the estimated gravitational field at different altitudes from (a) Eros and (b) Lutetia asteroids polygonal model surface with 300 thousand sphere packings*

5. Conclusion and Future Work

We presented a novel massively parallel algorithm to compute the gravitational field for arbitrary shaped small bodies like asteroids. The main idea is to represent the body by a polydisperse sphere packing. Based on this, we presented four methods to distribute the asteroid's total mass on to spherical mascons. Our algorithm outperforms the traditional polygon-based method by more than two orders of magnitude while achieving a similar accuracy. Compared to other mascon-based approaches, we achieve three times higher accuracy with the same number of mascons. These results qualify our algorithm perfectly for the application to physically-based simulation of space missions in virtual test beds including navigation,

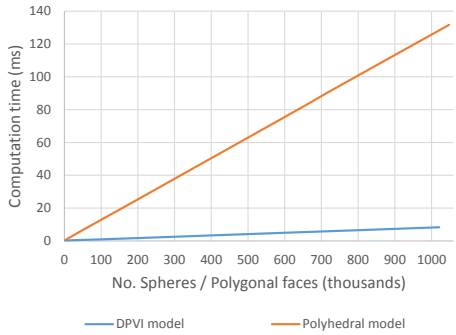

Figure 10: *Comparison of average times taken by DPVI spheres mascons model and polyhedral model to compute gravitational acceleration with regard to the number of spheres packings and number of polygons respectively.*

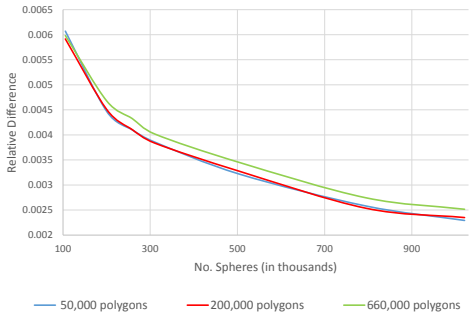

Figure 11: *Plot of estimated relative difference vs number of spheres using DPVI method considering shape model of 50 thousand, 200 thousand and 660 thousand polygonal faces*

guidance, and optimal path planning. Such applications do not only benefit directly from the performance gain of our algorithm, but they can also model completely new features, like arbitrary mass distributions inside the small bodies, which was unavailable from the traditional methods.

However, our algorithm also offers some interesting avenues for future works: for instance, it would be interesting to further investigate the sphere arrangement inside the sphere packing. The currently used Protosphere algorithm simply generates a greedy sphere packing but other arrangements could further improve the accuracy. Moreover, it would be interesting to solve also the inverse problem: i.e., to compute a mass distribution for a measured gravitational field of a small body. We are confident that our sphere packing approach in combination with an appropriate mathematical optimization scheme could overcome this challenge.

Acknowledgements

This work is based upon the project KaNaRiA, supported by the German Aerospace Center (DLR) with funds of the German Federal Ministry of Economics and Technology (BMWi) under the grant 50NA1318 and it is supported by the German Research Foundation (DFG) grant SFB 1320/R03

References

[BCJ*11] BALARAM J., CAMEROON J., JAIN A., KLINE H., LIM C., MAZHAR H., MYINT S., NAYAR H., PATTON R., POMERANTZ M.: Physics-based simulator for neo exploration analysis and simulation. *Pasadena, CA : Jet Propulsion Laboratory, National Aeronautics and Space Administration* (2011). 2

[KF13] KUCHYNKA P., FOLKNER W. M.: A new approach to determining asteroid masses from planetary range measurements. vol. 222, pp. 243 – 253. URL: http://www.sciencedirect.com/science/article/pii/S0019103512004496, doi:http://dx.doi.org/10.1016/j.icarus.2012.11.003. 3

[LJ09] LIM C. S., JAIN A.: Dshell++: A component based, reusable space system simulation framework. In *2009 Third IEEE International Conference on Space Mission Challenges for Information Technology* (July 2009), pp. 229–236. doi:10.1109/SMC-IT.2009.35. 2

[MKA*02] MILLER J., KONOPLIV A., ANTREASIAN P., BORDI J., CHESLEY S., HELFRICH C., OWEN W., WANG T., WILLIAMS B., YEOMANS D., SCHEERES D.: Determination of shape, gravity, and rotational state of asteroid 433 eros. *Icarus 155*, 1 (2002), 3 – 17. URL: http://www.sciencedirect.com/science/article/pii/S0019103501967533, doi:http://dx.doi.org/10.1006/icar.2001.6753. 6, 7

[NBC*08] NAYAR H., BALARAM B. J., CAMERON J., JAIN A., LIM C., MUKHERJEE R., PETERS S., POMERANTZ M., REDER L., SHAKKOTTAI P., WALL S.: *A Lunar Surface Operations Simulator*. Springer Berlin Heidelberg, Berlin, Heidelberg, 2008, pp. 65–74. URL: https://doi.org/10.1007/978-3-540-89076-8_10, doi:10.1007/978-3-540-89076-8_10. 2

[PWB08] PARK R., WERNER R., BHASKARAN S.: Estimating small-body gravity field from shape model and navigation data. American Institute of Aeronautics and Astronautics. 2

[RA12] RUSSELL R., ARORA N.: Global point mascon models for simple, accurate, and parallel geopotential computation. vol. 35, American Institute of Aeronautics and Astronautics Inc. (AIAA), pp. 1568–1581. doi:10.2514/1.54533. 2

[RJM*08] R.W.GASKELL, J.SAITO, M.ISHIGURO, T.KUBOTA, T.HASHIMOTO, N.HIRATA, S.ABE, O.BARNOUIN-JHA, D.SCHEERES: Gaskell itokawa shape model v1.0. hay-a-amica-5-itokawashape-v1.0. nasa planetary data system, 2008. 5

[R.W08] R.W.GASKELL: Gaskell eros shape model v1.0. near-a-msi-5-erosshape-v1.0. nasa planetary data system, 2008. 5

[Tar16] TARDIVEL S.: The limits of the mascons approximation of the homogeneous polyhedron. American Institute of Aeronautics and Astronautics Inc. (AIAA). doi:10.2514/6.2016-5261. 2, 3, 4, 6

[T.L13] T.L.FARNHAM: Shape model of asteroid 21 lutetia, ro-a-osinac/osiwac-5-lutetia-shape-v1.0, nasa planetary data system, 2013. 5

[TS14] TAKAHASHI Y., SCHEERES D. J.: Small body surface gravity fields via spherical harmonic expansions. vol. 119, pp. 169–206. URL: http://dx.doi.org/10.1007/s10569-014-9552-9, doi:10.1007/s10569-014-9552-9. 2

[WS96] WERNER R. A., SCHEERES D. J.: Exterior gravitation of a polyhedron derived and compared with harmonic and mascon gravitation representations of asteroid 4769 castalia. vol. 65, pp. 313–344. URL: http://dx.doi.org/10.1007/BF00053511, doi:10.1007/BF00053511. 2

[WZ10] WELLER R., ZACHMANN G.: Protosphere: A gpu-assisted prototype-guided sphere packing algorithm for arbitrary objects. In *ACM SIGGRAPH ASIA 2010 Sketches* (New York, NY, USA, Dec. 2010), ACM, pp. 8:1–8:2. URL: http://cg.in.tu-clausthal.de/research/protosphere, doi:http://doi.acm.org/10.1145/1899950.1899958. 3